Effects of benthic and hyporheic reactive transport on breakthrough curves

Antoine F. Aubeneau[1,3,4,5], Jennifer D. Drummond[1,6], Rina Schumer[2,7], Diogo Bolster[3,8], Jennifer L. Tank[4,9], and Aaron I. Packman[1,10]

[1]Department of Civil and Environmental Engineering, Northwestern University, Evanston, Illinois 60208 USA
[2]Division of Hydrologic Sciences, Desert Research Institute, Reno, Nevada 89512 USA
[3]Department of Civil and Environmental Engineering, University of Notre Dame, Notre Dame, Indiana 46556 USA
[4]Department of Biological Sciences, University of Notre Dame, Notre Dame, Indiana 46556 USA

Abstract: In streams and rivers, the benthic and hyporheic regions harbor the microbes that process many stream-borne constituents, including O_2, nutrients, C, and contaminants. The full distribution of transport time scales in these highly reactive regions must be understood because solute delivery and extended storage in these metabolically active zones control the opportunity for biogeochemical processing. The most commonly used transport models cannot capture these effects. We present a stochastic model for conservative and reactive solute transport in rivers based on continuous-time random-walk theory, which is capable of distinguishing and capturing processes not described by classical approaches. The model includes surface and subsurface storage zones with arbitrary residence-time distributions. We used this model to evaluate the effects of sorption and biological uptake on downstream solute transport. Linear or mildly nonlinear sorption in storage delays downstream transport without changing the fundamental shape of the breakthrough curves (BTCs). Highly nonlinear sorption isotherms can induce power-law tailing in stream BTCs. Model simulations show that sorption of commonly used solute tracers is not sufficient to explain the power-law tailing that has been observed in field tracer-injection studies, and instead, such tailing most probably reflects broad distributions of hyporheic exchange time scales. First-order biological uptake causes an exponential decline in in-stream tracer concentrations at the time scale of the uptake kinetics, thereby tempering power-law BTCs. The model can be used to calculate reach-scale reaction-rate coefficients in surface and subsurface storage from observed BTCs of co-injected conservative and reactive solutes, providing new capability to determine reaction-rate coefficients in storage zones with broad residence-time distributions.
Key words: hyporheic exchange, biogeochemistry, modeling

River networks transport the products of weathering from the continents to the oceans. Distributed physical, chemical, and biological processes control the downstream fluxes of dissolved and suspended materials. Streams and rivers transport, retain, and transform nutrients and other solutes (Bernhardt et al. 2003, Butman and Raymond 2011). Understanding the interactions between physical transport and biogeochemical processes is necessary to better estimate fluxes of biologically significant solutes and particles and to resolve environmental challenges, such as eutrophication and hypoxic zones at the mouth of major rivers (Turner and Rabalais 1994, Rabalais et al. 1996, Diaz and Rosenberg 2008).

Downstream solute transport is delayed because of incomplete mixing in the water column and exchange with slower regions like the hyporheic pore water. Traditional transport models, such as the advection dispersion equation (ADE), assume perfect mixing in the water column. In an ADE framework, solutes are transported at the mean velocity of the water column. The dispersion effect is meant to account for molecular diffusion, turbulent dispersion, and the range of velocities that exist in the stream. However, this model is inherently limited to systems with relatively narrow distributions of velocity, which is not the case for most stream or riverine flows. These models have been modified by including exchange from the main chan-

E-mail addresses: [5]aubeneau@gmail.com; [6]j-drummond@u.northwestern.edu; [7]rina.schumer@dri.edu; [8]diogo.bolster.5@nd.edu; [9]tank.1@nd.edu; [10]a-packman@northwestern.edu

DOI: 10.1086/680037. Received 27 November 2013; Accepted 11 September 2014; Published online 9 January 2015.
Freshwater Science. 2015. 34(1):301–315.

nel and well mixed storage reservoirs (Bencala and Walters 1983), which accounts for delays but misses the broad distribution of velocities inherent to these systems. In real streams, velocities are widely distributed and models using a single velocity that account for only a portion of the main-channel flow are not adequate. These models have been extended to include information about velocity distributions in various ways, such as memory kernels (Marion et al. 2008) or additional storage zones that incorporate additional time scales (Choi et al. 2000, Grant and Marusic 2011, Hensley and Cohen 2012).

Both physical and biogeochemical complexity are ubiquitous in streams. Transport properties and microbial communities are highly organized, influence one another, and often covary in space. Figure 1 schematically depicts a longitudinal section of a stream illustrating the coupling between velocity profiles and the biologically active benthic and hyporheic regions. Consumption of biologically important solutes (such as O_2 and NO_3^-) depends on microbial activity and on the time spent in the slow regions where microbes reside (Ensign and Doyle 2005, Zarnetske et al. 2011). Estimates of biogeochemical processing rates are obtained by comparing downstream transport of reactive and conservative solutes (Hauer and Lamberti 2011), so proper representation of residence-time distributions within bioreactive regions is important. Errors propagate and compound upon upscaling, so inadequate representations of transport at small scales, such as individual reaches, may produce misleading estimates of biogeochemical processes at large scales, such as whole watersheds. Similarly, diverse biogeochemical reactions and processes often are approximated with upscaled 1st-order rates, which do not capture the reality of coupled reactions involving various reactants and products.

We used 2 modeling techniques to illustrate the effects of distinct biophysical environments (water column, benthic region, hyporheic zone) on downstream breakthrough curves (BTCs). We used a flexible stochastic modeling framework that explicitly represents the interplay between transport and reactions in the core stream flow and storage regions characterized by any time scales of storage. We used numerical simulations to show effects of chemical sorption and biological uptake in specific biophysical environments on downstream solute transport, and we discuss the implications for estimating biogeochemical processing rates from whole-stream tracer injections. Our results clearly demonstrate the influence of local transport and biogeochemical processes on reach-scale biogeochemical signatures.

METHODS

Continuous-Time Random-Walk theory for solute transport in rivers

Random-walk models are powerful tools for representing transport of solutes in complex environments (Bouchaud and Georges 1990). Conceptually, solute plumes are broken into a finite number of particles representing discrete masses of solute, each of which then moves (and potentially reacts) based on a set of probabilistic rules designed to faithfully represent micro- and macro-scale pro-

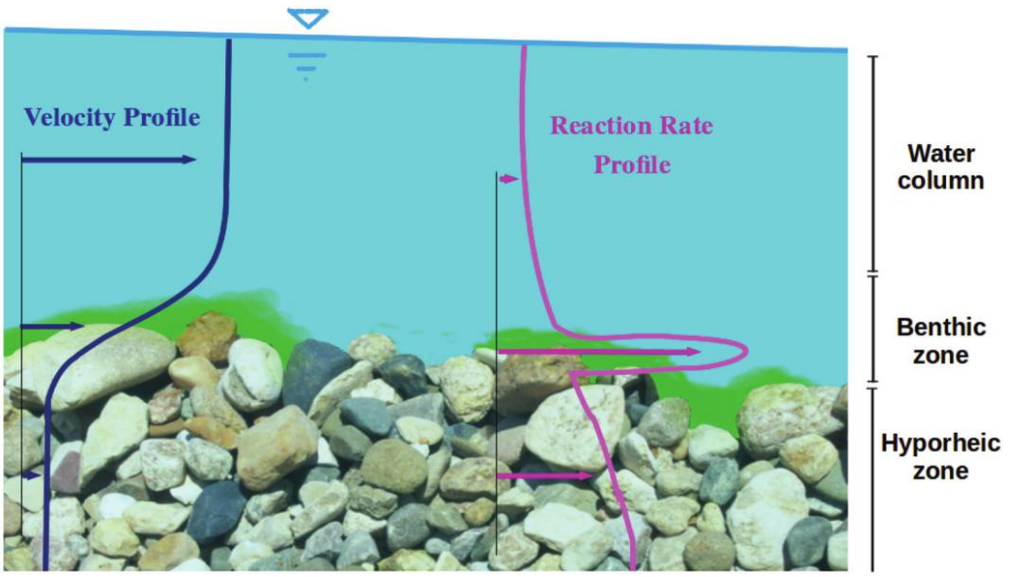

Figure 1. Schematic model illustrating the coupling between transport and biogeochemistry in streams and rivers. Arrows represent a global value for the water column, the benthic zone, and the hyporheic zone (from top to bottom). The benthic and hyporheic zones are both biogeochemical hotspots with active biofilms (in green, benthic biofilm) and regions of slow transport, creating a competition between mass delivery from the flow and consumption rates in biofilms. The rate profile shows sharp contrasts between regions.

cesses. The mass parcels of tracer move via a series of steps, sampled from a probability distribution. When the step-distributions are narrow, the resulting model yields classic diffusive (or dispersive) transport. A typical metric that quantifies whether the system behaves in this manner is the variance of the spatial distribution of solute mass, which characterizes the spatial extent of a solute plume. If this variance grows linearly in time, the system is said to behave in a Fickian manner and classical ADE approaches are likely to work well.

However, in rivers, these distributions may not be narrow because solutes can experience very low water velocities and long residence times in surface dead zones or in the subsurface. Extensive regions of near-0 velocity coupled with fast flow regions in the main channel can violate the assumptions of the standard Fickian dispersion model (Metzler and Klafter 2000). For this case, the variance of the spatial distribution grows nonlinearly in time, a behavior called anomalous (or nonFickian) transport, i.e., transport that does not follow the predictions of classical ADE theory.

A rich family of models exists that relax these assumptions. One such model is the Continuous-Time Random-Walk (CTRW), which can account for anomalous transport emerging from the broad range of velocity and time scales. The CTRW can be described mathematically by the equation (Berkowitz et al. 2006, Boano et al. 2007):

$$\frac{\partial C(x,t)}{\partial t} = \int_0^t M(t-t')\left[U\frac{\partial C(x,t')}{\partial x}dt' + K\frac{\partial^2 C(x,t')}{\partial x^2}\right]dt', \quad \text{(Eq. 1)}$$

where, in Laplace space, M is

$$\tilde{M}(u) = u\bar{t}\frac{\tilde{\psi}(u)}{1-\tilde{\psi}(u).} \quad \text{(Eq. 2)}$$

In these equations, U and K represent the velocity and dispersion in the water column, C is concentration, x is distance, t is time, t' is a dummy time variable, $\bar{t}$ is the advective time in the water column, and u is the Laplace variable. M is a memory function that accounts for time delays, which in Eq. 2 is written in Laplace space, a commonly used mathematical transformation that makes calculations considerably easier. $\tilde{\psi}(u)$ represents the residence-time distribution (RTD). It quantifies the probability that a parcel of water entering a given location in the system at time 0 will leave at some later time t. When $\tilde{\psi}(u)$ is a narrow distribution (e.g., exponential), the model is equivalent to the classical ADE model. However, residence times in many streams are not narrowly distributed. For broad RTDs (heavy-tailed power laws, gamma functions), the model is able to represent commonly observed anomalous transport. Thus, $\tilde{\psi}(u)$ dictates the emergent behavior of the system and must be chosen carefully to represent all pertinent physical processes.

Solute exchange between the main channel and the benthic or hyporheic regions can be readily included in $\tilde{\psi}(u)$ following the approach of Margolin et al. (2003) and Boano et al. (2007), which are adapted here to account for different RTDs associated with different stream compartments:

$$\tilde{\psi}(u) = \tilde{\psi}_0[u + \Lambda_B - \Lambda_B\tilde{\varphi}_B(u) + \Lambda_H - \Lambda_H\tilde{\varphi}_H(u)]. \quad \text{(Eq. 3)}$$

$\tilde{\psi}(u)$ is the RTD for the entire system and accounts for the likelihood of all possible exchanges from the water column to immobile regions. $\tilde{\psi}_0$ is the RTD for the water column, $\tilde{\varphi}_B$ is the RTD in the benthic reactive region, and $\tilde{\varphi}_H(u)$ is the RTD in the hyporheic reactive region. Λ_B and Λ_H are exchange rates to the benthic and hyporheic zones respectively. Thus, the $\tilde{\varphi}$ terms represent how long solute will reside in a given storage zone, whereas the Λ terms represent how quickly exchange will occur between them. Note, mathematically, that $[u + \Lambda_B - \Lambda_B\tilde{\varphi}_B(u) + \Lambda_H - \Lambda_H\tilde{\varphi}_H(u)]$ is the modified argument of the function $\tilde{\psi}_0$.

The choice of each of these distributions and exchange rates typically is motivated by a combination of physical arguments and experimental observations. Based on experimental evidence (e.g., Haggerty et al. 2002, Drummond et al. 2012, Stonedahl et al. 2012), we set $\tilde{\psi}_0 = \frac{1}{1+u}$, and used exponential RTDs in the benthic zone and power-law RTDs in the hyporheos. $\tilde{\psi}(u)$ can be obtained using a variety of other approaches, such as deconvolution (Cirpka et al. 2007, Payn et al. 2008) or physical models (Stonedahl et al. 2012). Calculations are done in the Laplace domain because convolution integrals, such as the one in Eq. 1, are difficult to calculate or compute and disappear under the Laplace transformation. Another important feature of Eq. 1 is that its structure is complex, but it is a linear equation, i.e., each term in Eq. 1 depends only on C and not on arbitrary powers of C. Because of the principle of linear superposition, linear equations have the great benefit that they can be solved for any initial condition or with any arbitrary source terms by solving for only the case of a pulse injection (Arfken and Weber 1995). The solution to the differential equation with pulse initial condition is the Green's function, and solutions for the same equation with more complex sources (e.g., periodic, step, continuous) can be obtained by combining (more precisely by convolving) the new initial condition and the Green's function solution. Thus, understanding the simple case of a pulse initial condition provides all information needed to understand more complicated solute-transport problems.

Particle-tracking simulations

The CTRW described in the previous section simulates downstream plume evolution through use of a properly structured travel-time distribution (Eq. 3), rather than by explicitly resolving small-scale physical processes. To model such processes explicitly, a smaller-scale model that resolves the features of interest is needed. To validate analytical solutions and to observe solutions that are not analytically tractable, we used a particle-tracking method that resolves specified hydrodynamic and biogeochemical processes, such as the spatial variation of flow velocities and uptake rates (Fig. 1).

We simulated solute motion in the downstream cross-section of a reach that was 0.3 m deep, had a bed slope of 0.5%, and median particle diameter in the bed sediment of D_{50} = 1 cm. We solved the transport problem via classical random-walk methods, which differ from those of the CTRW described above (Delay et al. 2005) in that they resolve the motion of solute as it moves vertically and horizontally in the stream; i.e., the model provides the full spatial distribution of solute and not just information on how it is distributed in the downstream direction. We distributed numerical particles, representing parcels of solute mass, over the water-column depth at a location $x = 0$ and at time $t = 0$ to simulate a pulse injection and ran the model for 1×10^5 s. We treated the top and bottom boundaries as no flux, reflective boundaries.

We carried out parallelized simulations with 1,000,000 particles for each simulation. We then computed BTCs at locations 100, 200, 300, and 400 m downstream to capture typical reach lengths in field experiments. BTCs were obtained by logging the mean passage time of each particle across a given measurement location.

Following classical theory for open-channel flow (Raudkivi 1979, Brutsaert 2005), we modeled the in-stream velocity profile in the surface water with a log-law distribution:

$$v(y+) = \bar{v} + \frac{v^*}{k} + \frac{2.3}{k} v^* \log\left(\frac{y}{d}\right), \qquad \text{(Eq. 4)}$$

where $\bar{v}$ is the mean velocity in the water column, $v^* = \sqrt{(gds)}$ is the shear velocity, g is gravity, d is the water column depth, s is the bed slope, k is the Von Karman constant, and y is the relative position in the water column from the stream bed. The mean surface velocity is $30\sqrt{(sd)}$.

To represent subsurface flow beneath the open channel, we used Darcy's law for flow through porous media, where the porewater velocity was calculated as ΦKs, where Φ is the porosity and K is the hydraulic conductivity. Porosity was held at 30%, representative of many natural porous media, and $K = 100\ D_{50}{}^2$ (Bear 1972, Uma et al. 1989). In the water column, dispersion coefficients were calculated as $D = \rho u^* \frac{\partial y}{\partial u}$ (Fischer 1979). In the subsurface, the dispersion is proportional to the velocity and dispersivity, taken as D_{50} (Bear 1972).

Sorption

Sorption of solute to the porous material underlying the open channel can delay downstream transport by holding solute back relative to the mean flow of the system. Linear sorption is most often modeled with a retardation coefficient, which quantifies delay in transport relative to that in an equivalent system without sorption. Margolin et al. (2003) showed that for solutes undergoing linear sorption, Eq. 3 becomes:

$$\tilde{\psi}(u) = \tilde{\psi}_0[R_0(u + \Lambda_B - \Lambda_B R_B \tilde{\varphi}_B(u) + \Lambda_H - \Lambda_H R_H \tilde{\varphi}_H(u))], \qquad \text{(Eq. 5)}$$

where R_0 is retardation in the water column, and R_B and R_H are the retardation factors for the benthic and hyporheic zones, respectively.

The assumption of linear sorption is convenient, but it fails in many instances because porous material may have a limited capacity to sorb all of the solute passing through it. This limitation is particularly important at high solute concentrations where the amount of solute exceeds the sites available for binding. This situation typically results in a nonlinear relationship between sorbed and mobile solute concentrations. No simple analytical solution exists for the CTRW with nonlinear sorption (Margolin et al. 2003). Instead, for this case, we must solve the governing equations numerically. A common representation of nonlinear sorption is the Freundlich isotherm:

$$C_S = FC^n, \qquad \text{(Eq. 6)}$$

where C_s is the concentration of the adsorbed solute in mass of adsorbate/mass of adsorbent, F is the Freundlich constant, and n is an exponent describing the nonlinearity of the relationship. When $n = 1$, the linear sorption model described above is recovered. We partition the concentration between a dissolved and sorbed state using this equation at each time step. Mathematically, the residence time is then updated to account for the proportion of the mass in storage that is adsorbed (assuming transport and sorption are independent), so that we simply multiply the probability of moving by the probability of not being adsorbed. We calculate the mobile-zone concentration taking into account this new waiting time and update the boundary condition for the next time step. To test this numerical procedure, we verified that it reproduced results from equivalent finite difference solutions of an ADE with nonlinear sorption and a storage zone with nonlinear sorption.

Biological uptake

We also wanted the model to account for biological uptake. Biological uptake is the rate of mass removal from the water column/unit bed area (U, with units M L^{-2} T^{-1}). It also can be expressed as a nutrient uptake velocity, v_f(L/T) = U/C (M/L^3), or a 1st-order mass transfer rate k (/T) = v_f/d (Newbold et al. 1983, Stream Solute Workshop 1990).

The RTD in a system, $\varphi(t)$ in Eq. 2, is the probability that solute entering the system at time 0 will leave at time t. However, if that solute undergoes degradation following 1st-order kinetics, it may degrade before it has time to leave. The probability that it degrades over a time t is exponential and given by $e^{-k_x t}$. k_x is a 1st-order rate constant and can differ for the water column, benthic zone, and hyporheos. Therefore, Eq. 1 can be recast to account for reactions:

$$\psi(t) = \psi_{0(t)} e^{-k_0 t} \qquad \text{(Eq. 7)}$$

and

$$\mathcal{L}(\psi(t)e^{k_0 t}) = \tilde{\psi}_0[u + \Lambda_B - \Lambda_B \mathcal{L}(\varphi_B(t)e^{-k_B t}) + \Lambda_H - \Lambda_H \mathcal{L}(\varphi_H(t)e^{-k_H t})], \qquad \text{(Eq. 8)}$$

where k_0, k_B, and k_H are the water-column, benthic, and hyporheic uptake rate coefficients and $\mathcal{L}$ is the Laplace transform operator. In the highly resolved particle-tracking simulations, the degradation rate is simulated stochastically by assigning each particle a probability of decaying depending on its location.

RESULTS

In this section, we use both the analytical CTRW model and the particle-tracking model to demonstrate how the various mechanisms described above influence BTCs so that specific observations can be attributed to specific transport or uptake behaviors. In all cases, for the reasons outlined above, we consider a pulse-injection initial condition because this situation provides all pertinent information in the system. For ease of visualization, we normalized the results by the maximum observed concentration at the sampling station. Equivalent results for continuous injections and the nonnormalized data can be found in Figs S1–S9. We also present all the results in logarithmic space where exponentials and power laws are easily distinguished, except in Fig. 8, which is in linear space.

Conservative solutes

First, we explored the effect of varying benthic-zone parameters on in-stream BTCs using an exponential RTD. Figures 2A and S6A demonstrate the effect of changing the mean residence time in the benthic zone with a fixed exchange rate between the main channel and benthic zone. As mean benthic residence time increases, asymmetry in the observed BTC also increases with a stronger exponential tail. This asymmetry represents the fact that the longer solute is held in the benthic zone, the longer it will take for all of the solute to reach a downstream location. Figure S1A shows the BTC for a continuous injection, where the effect of longer residence is a delay in the time to the equilibrium plateau. Figures 2B, S1B, and S6B show the effects of varying the exchange rate between the main channel and the benthic reactive zone (Λ_B). As the exchange rate increases, the BTCs become more skewed, reflecting the fact that as the total mass transferred to the benthos increases, more time is required for all of the mass to break through at a given point. As the exchange rates become smaller and smaller, the behavior in the BTC converges to a behavior consistent with the ADE because most of the mass never reaches the benthic region. However, after more time, or equivalently more distance downstream, the total mass transferred to the benthos will increase so that even small transfer rates may have significant effects at larger scales. Similar to the effect of increasing mean residence time, an increase in transfer rates affects continuous-injection BTCs by delaying the time until the equilibrium plateau is reached (Fig. S1B).

Figures 3A, S2, and S7 show how BTCs are influenced by the parameters associated with the hyporheic storage RTD. In all cases, this RTD is described by a power law, characterized by a power-law exponent β (i.e., $\varphi(t) \sim t^{-\beta}$). The smaller the β, the heavier the RTD tail, which physically means a greater likelihood of extreme residence times, i.e., some solute is more likely to spend a much longer time in the hyporheic zone than most solute particles. The specific value of β will be a reflection of the transport processes that occur in the hyporheic zone and can either be inferred from experimental data or based on physical arguments. Our results show a range of $0 < \beta < 1$. The upper limit of $\beta < 1$ is chosen because, for $\beta > 1$, behavior converges to the classical ADE. As β decreases, the effects of the hyporheic zone become more pronounced. Specifically, as β decreases, tailing effects are evident at higher concentrations and the slope of the tail decreases. In fact, the BTC slope on a log–log plot is $-\beta - 1$ (Schumer et al. 2003). Thus, observation of more pronounced tails for conservative tracers suggests that hyporheic processes (e.g., biogeochemical reactions) may be of greater importance in a system as a whole.

Figures 3B, S2B, and S7B demonstrate the effect of varying the exchange rate between the main channel and the hyporheic storage. As with the benthic exchange rates in Fig. 2, as the exchange rate increases, more mass enters the hyporheic zone/unit time, but because the return rate to

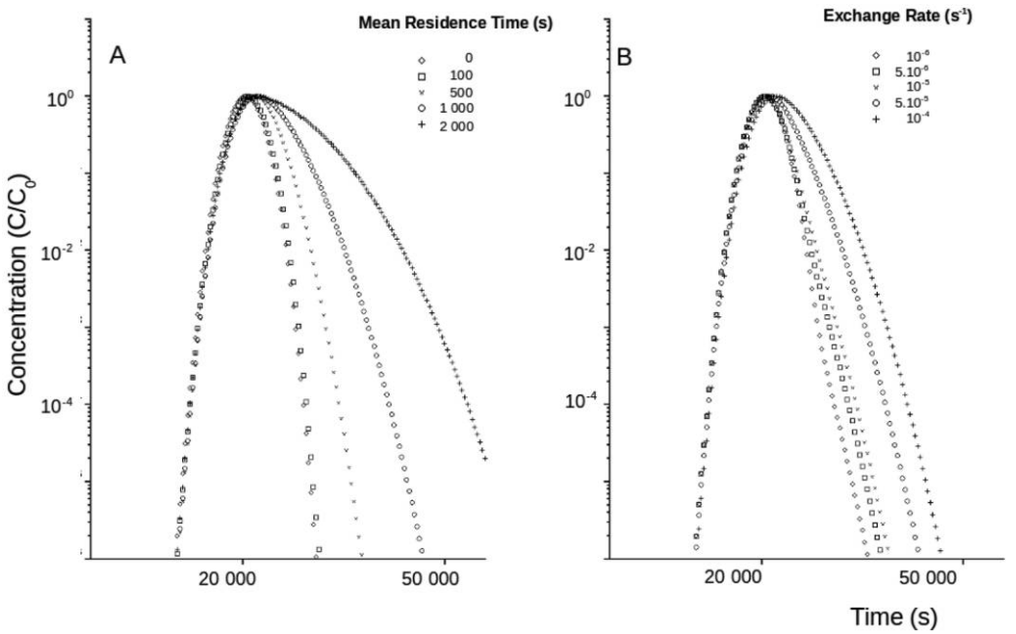

Figure 2. Breakthrough curves showing the effects of the benthic-zone residence-time distribution (RTD) and exchange rate (Λ_B) on concentration (C/C_0). A.—$\Lambda_B = 1 \times 10^{-3}$/s and the mean of the exponential RTD is varied from 0 s (corresponding to an advection dispersion equation [ADE] model) to 2000 s. B.—Mean RTD = 1000 s and Λ_B is varied from 1×10^{-6} to 1×10^{-4}/s. In all cases, the velocity u is 0.1 m/s and the dispersion coefficient $D = 0.4$ m/s^2.

the main channel is controlled strictly by the RTD, more solute is held behind the mean flow and tailing occurs earlier. However, the slope of the late-time BTC does not change and is entirely dictated by the value of the power-law RTD exponent. The specific value of the exchange rate will depend on the nature of the flow at the interface between the hyporheic zone and the open channel. For example, greater turbulence or roughness can result in greater exchange rate. The specific value can be estimated from data or physical models that capture these processes.

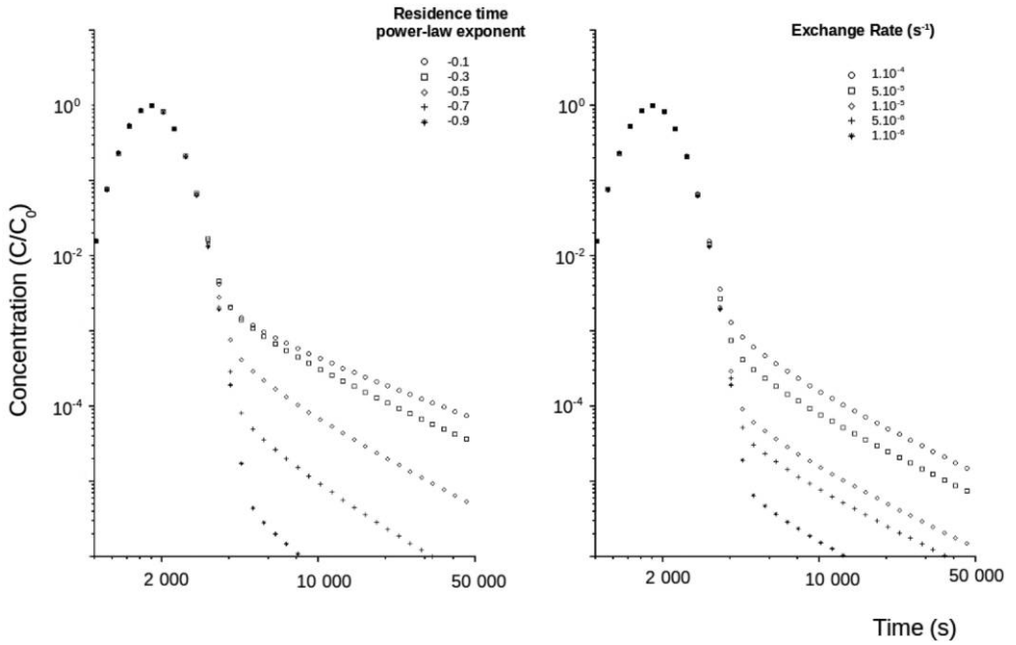

Figure 3. Breakthrough curves (BTCs) showing the effects of hyporheic-zone residence-time distribution and exchange rate (Λ_H) on concentration (C/C_0). A.—$\Lambda_H = 1 \times 10^{-4}$ and RTD power-law exponent (β) varies between −0.1 and −0.9. B.—β = −0.4 and Λ_H varies between 1×10^{-6} and 1×10^{-4}/s. The slope of the BTCs on these log–log plots is β. u and D are as in Fig. 2.

Sorption

Linear sorption In a homogeneous domain, linear reversible sorption produces retardation. It shifts the BTC in time and delays the arrival of solute at a given location, but does not change the shape of the BTC. However, in streams, retardation may vary in space and may be different in each storage zone. Under baseflow conditions, sorption commonly occurs only in the benthic and hyporheic regions and not in the water column. In this case, the BTC peak is not retarded, but the BTC tail extends further in time. In other words, in heterogeneous domains, the in-stream BTCs of reversibly sorbing solutes do not simply shift in time. The peaks predominantly reflects mass that has remained in the open channel and not undergone sorption, whereas the tails represent mass that has entered the benthic and hyporheic regions where retardation does occur.

Figures 4A, B, S3A, B, and S8A, B highlight the effects of linear retardation. An increase in the linear retardation coefficient in the benthic region leads to a widening of the exponential tail, reflecting the fact that retardation in the benthic zone results in greater residence times there, delaying downstream transport (Fig. 4A). Linear retardation in the hyporheic zone does not affect the slope or shape of the BTC tail, but does affect timing of the onset of tailing. As the retardation coefficient increases, tailing appears later and at lower concentration (Fig. 4B). The total mass returning from the hyporheic zone is unaffected. It simply returns over a longer period.

Nonlinear sorption Figures 5A, B, S4A, B, and S9A, B show BTCs affected by nonlinear sorption in the hyporheic zone. Nonlinear sorption can induce power-law BTC tails, but only for strongly sorbing solutes. Increasing nonlinearity in the sorption isotherm increases the time spent in the hyporheos. The slope of the power-law tail increases with increasing Freundlich exponent (Fig. 5A). It appears that only solutes with strong nonlinear sorption (exponent <0.5) fall in that range. For a Freundlich exponent of 0.4, corresponding to a slope of ~−2, the mass affected by the tailing is so small that it does not appear over 5 orders of magnitude of concentration data, which is more than the dynamic range of commonly used fluorometric methods (Fig. 5B).

Uptake

Last, we demonstrated the influence of uptake in the main channel or hyporheic zone on downstream transport by varying the 1st-order uptake rate coefficient between 0 (conservative solute) and 0.005/s. This range spans from no uptake to a relatively high rate of NO_3^- uptake (Mulholland et al. 2008). Increasing uptake in the main flow channel causes the entire BTC concentration to decrease in a manner proportional to the uptake rate, but it does not affect the overall shape or structure of the BTCs (Figs 6A, S5A).

When uptake is included in the hyporheic zone only (Figs 6B, S5B, S10B), no effect on the early peak of the BTC is observed because the early peak accounts for sol-

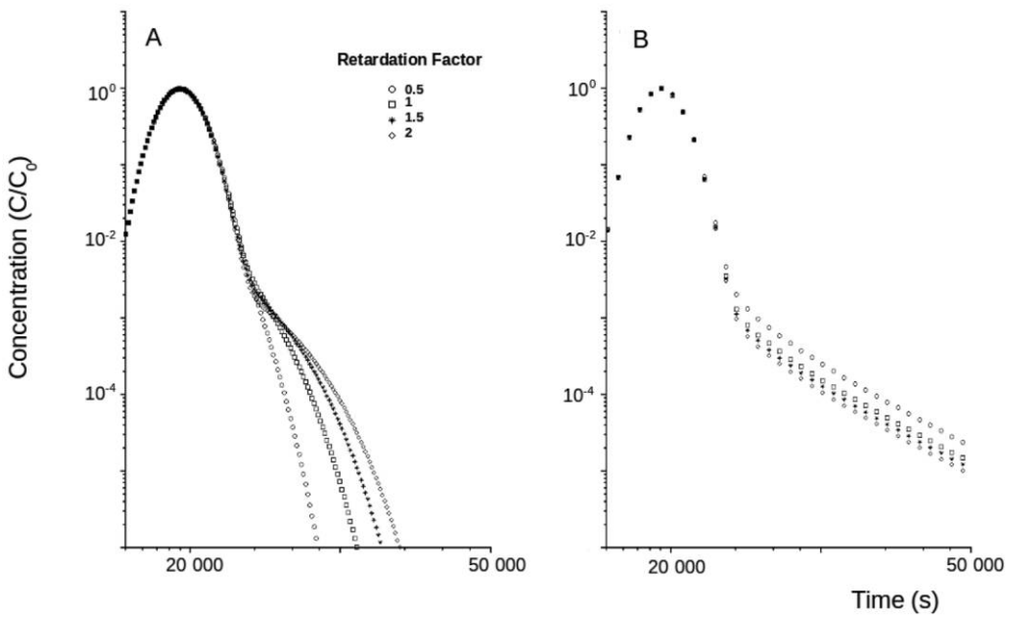

Figure 4. Breakthrough curves (BTCs) showing the effects of linear sorption in the benthic and hyporheic zones on concentration (C/C_0). A.—The retardation factor associated with exponential residence-time distribution with benthic=zone exchange rate (Λ_B) = 1×10^{-4} affects the width of the BTC tail. B.—The retardation factor associated with power-law residence-time distribution with an exponent $\beta = -0.4$ in the hyporheic zone affects the timing of the onset of tailing. u and D are as in Fig. 2.

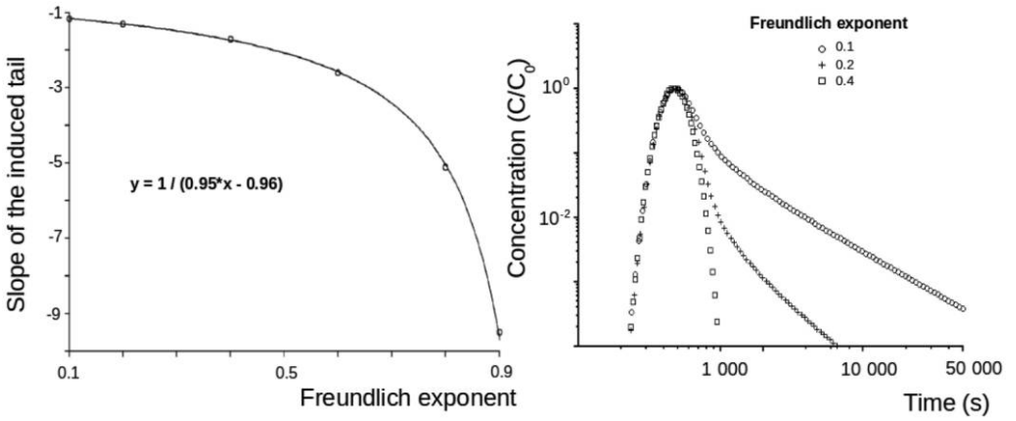

Figure 5. Breakthrough curves (BTCs) showing the effects of nonlinear sorption in the hyporheic zone on concentration (C/C_0). A.—Relationship between the Freundlich exponent and the slope (β) of the observed power-law residence-time distribution. B.—BTCs observed for different Freundlich exponents. *u* and *D* are as in Fig. 2.

ute that has never entered the hyporheic zone. The influence of hyporheic uptake is evident primarily in the tails of the BTC. For 0 uptake, the power-law tail is strong and persistent. As uptake increases, this tail is cut off earlier as more mass is consumed in the hyporheic zone and never returns to the main channel. The cutoff in the power-law tail reflects competition between the kinetics of biogeochemical processing and the power-law residence time. The shape of the curve is a tempered power law (Meerschaert 2013). We reproduced the same tempering effect with the particle-tracking model to compare effects of conservative or reaction kinetics in the hyporheic zone (Fig. 7). The conservative solute BTC shows a behavior very similar to that obtained with the CTRW model with hyporheic exchange (e.g., Fig. 3A, B) with a power-law exponent of –1.6 that emerges naturally from the small-scale physics. For the reactive solute, this power law is tempered at an exponential rate as in the CTRW analytical model results (e.g., Fig. 6A, B). The decay rate of the exponential function corresponds exactly to the reaction rate coefficient in the hyporheic zone. In other words, if one can measure the BTC for a conservative and a reactive tracer for sufficiently long times to observe the hyporheic signal, the difference between the power law

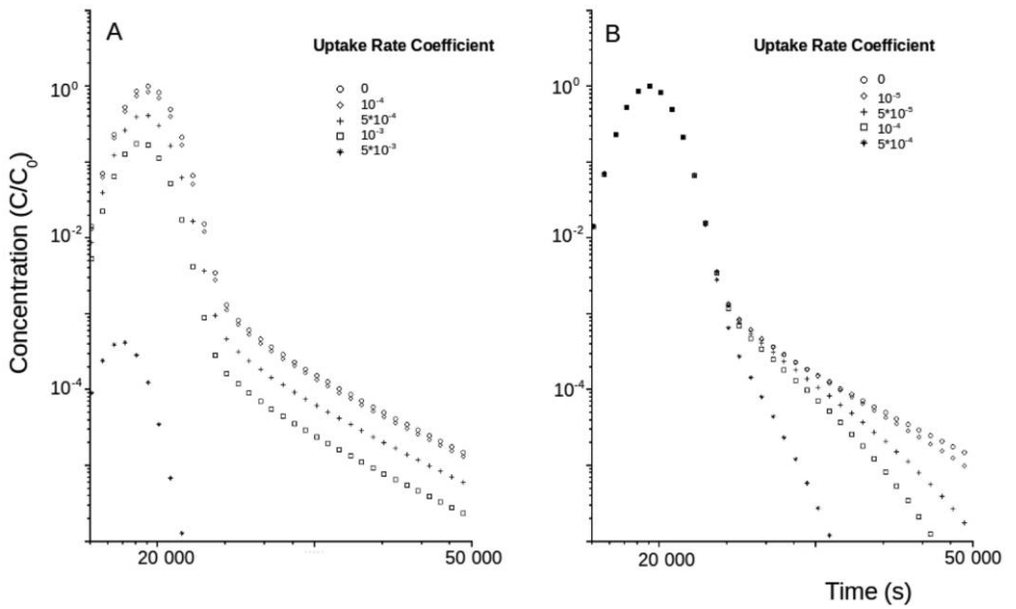

Figure 6. Breakthrough curves (BTCs) showing the effects of a 1st-order uptake on concentration (C/C_0). A.—Increasing uptake in the main channel causes BTC concentration to decrease in a manner proportional to the uptake rate. B.—Uptake in the hyporheic zone tempers power-law BTCs caused by a power-law residence-time distribution. *u* and *D* are as in Fig. 2.

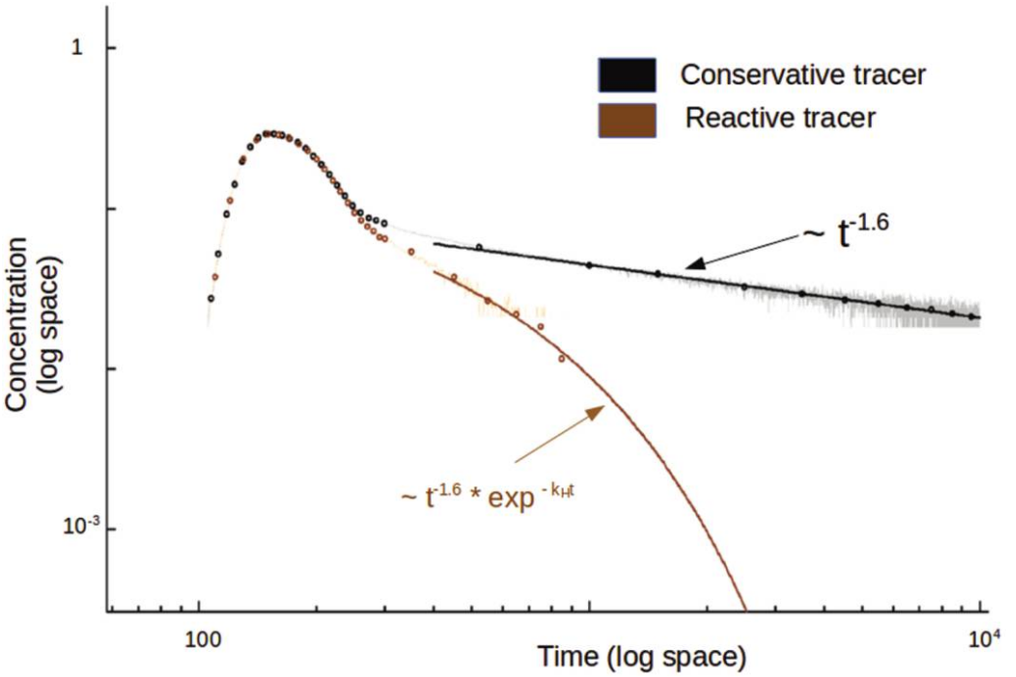

Figure 7. Breakthrough curves (BTCs) showing the effects of a 1st-order uptake in the hyporheic zone (synthetic data, log space). Hyporheic uptake is reflected in the tempering rate of the power-law residence-time distribution. Light grey shows the conservative particle-tracking results, light brown the bioavailable particle-tracking results, the bold markers show the smoothed results, and the lines show the scaling in the tail of the BTC, reflecting hyporheic storage and uptake signatures.

and the tempered power law provides a direct measure of the hyporheic reaction rate coefficient. These synthetic data demonstrate the utility of the CTRW model for effectively describing the large-scale dynamics without the need for resolving all small-scale features.

At high uptake rates, the entire mass of solute that enters the subsurface can be consumed as long as the concentration is not so high that it saturates the system. When k_H is much greater than Λ_H, the observed BTC resembles an ADE solution in all aspects except the mass balance, which decays exponentially with downstream distance. In this case, the overall kinetics of uptake at the reach scale are transport limited, and the exchange rate between the surface and subsurface controls the proportion of solute removed. If transport limitations associated with hyporheic exchange are not considered, then the exponential removal of the reactive solute from the stream can be misinterpreted as characterizing the rate constant for 1st-order biological uptake instead of the rate of hyporheic exchange flow. To highlight this point, we ran particle-tracking simulations that explicitly modeled transport in a spatially variable flow field with uptake in all of or a subset of the open channel, benthic, and hyporheic regions. We present 3 sets of BTCs at 4 locations for: 1) a conservative system, 2) a well mixed system with a uniform degradation rate over the entire domain, and 3) a heterogeneous system in which uptake affects only the benthic layer but not the water column (Fig. 8). Of the 3 scenarios, the conservative BTCs have the highest peak concentrations and broadest BTCs, as one would expect. For the well mixed case, mass is removed from the system without regard for how it is spatially distributed in the column (i.e., this model does not distinguish between mass in the main channel and the hyporheic zone, which react differently), and only reaction kinetics control the amount of mass that is removed along the reach. Conversely, when uptake occurs only in the benthic layer, the BTC shape depends on the reaction kinetics and the transport into and out of the reactive zone. As a result, the BTC peak is shifted to the left with respect to the well mixed case, because slower moving mass is more likely to have resided in the reactive regions, whereas faster moving mass has resided in the unreactive water column. Most importantly, the well mixed case is not merely a rescaled form of the case with only benthic reactions that could be described with some modified reaction rate, but has a fundamentally different shape.

DISCUSSION

Model formulation

The CTRW model framework can include reactive solute transport in the stream, benthos, and hyporheic zone. The model is sufficiently general, in that it allows the required separation of transport time scales between the

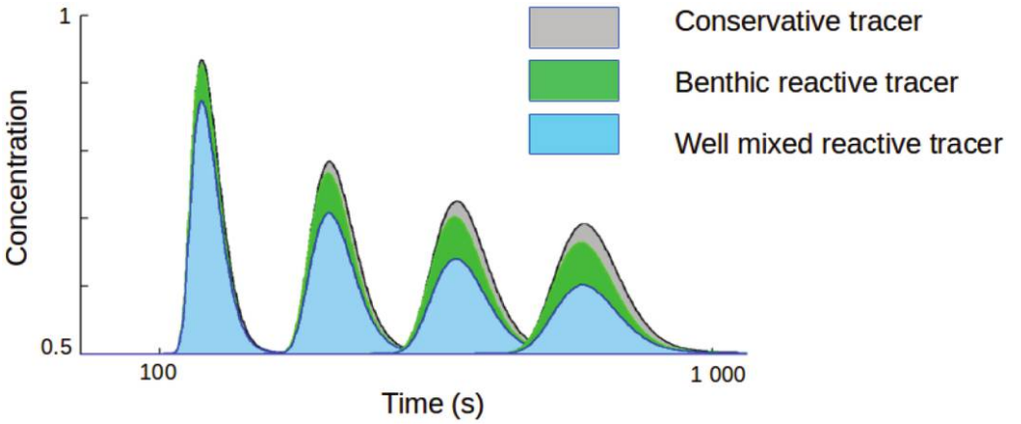

Figure 8. Breakthrough curves (synthetic data) showing the effects of a 1st-order uptake throughout the water column (blue) and in the benthic layer (green). Note the linear axis scale. The plume of solute is measured downstream of an injection at 100, 200, 300, and 400 m. A tracer that reacts only in the benthos appears to be faster (and has a different shape) than the tracer that reacts through the entire water column, which simply scales the conservative concentration profile.

main river flow and the benthic and hyporheic zones and enables separate evaluation of the effects of biogeochemical processes in each of these reactive regions (Fig. 1). Nevertheless, some of the model's assumptions may not be directly applicable to all rivers, and we discuss some of these limitations below.

Rivers with coarse sediments where subsurface velocities are similar to in-stream velocities may violate the assumption of separation of time scales, but the model can be modified readily to address such issues. Moreover, in-stream storage is widely distributed in space and occurs at many locations around rough channel boundaries. Transverse mixing in rivers also is much slower than vertical mixing because rivers are wider than deep, so that hours may be needed to achieve complete mixing (Fischer et al. 1979). Thus, many processes contribute to the slow spreading of solutes. Nevertheless, separation of in-stream, benthic (interfacial), and hyporheic (subsurface) processes is convenient to understand reactive transport because biological communities and water velocities are very different in these 3 compartments (Battin et al. 2008).

The CTRW model formulation that we used assumes that sufficient mixing has occurred for solute motion and residence times in immobile zones to be independent of one another and stationary, i.e., their distributions do not change in space or time. These assumptions make the solution tractable and are expected to be applicable to many streams and rivers. However, if transport must be modeled over smaller spatial scales, displacements can be correlated in time; i.e., slow moving parcels of water will continue to move slowly for long periods of time and fast moving ones will continue to move quickly for long periods of time. CTRW have been generalized even further to incorporate such effects (e.g., De Anna et al. 2013). Downstream changes in channel morphology, hydrology, chemistry, or ecology also are not currently included in the model, but with sufficient information could be included. Furthermore, we assume that the surface and the reactive zones are homogeneous, such that sorption and uptake can be represented by single reaction parameters and that these reaction parameters are independent of transport rates. Physical heterogeneity of the subsurface has been considered in this context by Salehin et al. (2004), Boano et al. (2007), and Sawyer et al. (2011) and can be readily included in the model framework presented here as long as it remains independent of reaction parameters. Subsurface heterogeneity extends RTDs and the tails of in-stream BTCs (Boano et al. 2007), and the power-law BTC tails that have been observed in the field probably reflect spatial variability in stream velocities, channel morphology, and subsurface structure.

Biogeochemical processes covary with sediment structure and porewater flow. Most notably, sedimentary microbial communities are structured according to redox gradients. In stream beds, these gradients are established primarily by O_2 delivery from the water column, production by photosynthesis at or near the bed surface, and heterotrophic metabolism in benthic periphyton and the underlying hyporheos. Thus, higher-velocity regions of pore water that are better connected hydraulically to the stream will have greater O_2 influx and will support more aerobic metabolism. In contrast, lower-velocity regions that are more isolated from the overlying flow, e.g., pockets of fine deposits in coarser and better-oxygenated material and the interior of biofilms, will tend to support anaerobic metabolism. The interaction of transport, sediment structure, and microbial communities can produce complex coupled biogeochemical dynamics (Arnon et al. 2007, O'Connor and Hondzo 2008, Bardini et al. 2013). More generally, biogeochemical cycles are coupled together and to the geomorphology of the stream ecosystem. Thus, the 1st-order uptake rates are a strong simpli-

fication of actual processes. Reach-scale estimates that combine all of these processes oversimplify system dynamics and can produce misleading results that inappropriately conflate transport and biogeochemical processes.

Despite possible limitations, the simulations presented here illustrate the general effects of residence times, sorption, and 1st-order uptake in contrasting biogeoreactive regions on downstream solute transport. The results show that interpretations of reach-scale biogeochemical dynamics require explicit accounting of both biogeochemical and transport processes. The interplay between stream transport, fluxes to and from regions where biogeochemical transformations occur, and local transformation and uptake rates is important at all scales in rivers because of the high spatial variability inherent in fluvial systems. Moreover, larger-scale spatial variability must be accounted for when attempting to simulate dynamics of whole watersheds because downstream changes in channel morphology, stream flow, sedimentary conditions, and ecosystem structure that are ignored at the scale of small experimental reaches certainly will be important at the scale of entire river networks.

Interpretation of tracer-injection results

Measuring a conservative solute with enough sensitivity and accuracy for a long enough period of time is a practical challenge. Flux calculations using, e.g., the model of Elliott and Brooks (1997), or computational fluid dynamics (Cardenas and Wilson 2007, Sawyer and Cardenas 2009) show that flux into the subsurface generally is orders of magnitude lower than the solute flux downstream, except for steep streams underlain by coarse, highly permeable sediments. Therefore, the onset of BTC tailing often is several orders of magnitude below the injection concentration. In most situations, the instrumentation used to measure the conservative solute will have to be able to resolve several orders of magnitude of concentrations to avoid losing the signal in a noisy background (Drummond et al. 2012).

Incomplete mixing in the main channel dominates at early times, so late-time sampling is necessary to detect the hyporheic signal. Benthic delays created by slower velocities in that region appear in the BTCs, but the hyporheic signal is rarely recorded. The extended travel times through the benthic zone (or incomplete surface mixing) may be mistaken for a hyporheic signal and data misinterpreted. A mass–balance for a system with storage zones with exponential RTDs shows that

$$\frac{C_r}{C_0} = \sum \Lambda_i \times L/v \times e^{-k_i t}, \qquad \text{(Eq. 9)}$$

where C_r is the measured concentration at the surface, L is the reach length, v is the streamwise velocity, and i is either the benthic or hyporheic reactive zone. The time when the measured signal from the benthic storage is much smaller than the hyporheic signal, e.g., <10%, can be calculated as:

$$\Lambda_B e^{-k_B t} < 0.1 \Lambda_H e^{-k_H t}. \qquad \text{(Eq. 10)}$$

Taking logarithms and rearranging, we obtain the hyporheic signal time:

$$t > \frac{\log(\Lambda_B) - \log(\Lambda_H) - \log(0.1)}{k_B - k_H}. \qquad \text{(Eq. 11)}$$

Considering a typical case where exchange with the benthic zone is much greater than hyporheic exchange and the mean residence time in the benthos is much smaller than in the hyporheos, we obtain the following approximation:

$$\frac{C_r}{C_0} \approx \Lambda_H e^{-f_H t} \pm 10\%, \qquad \text{(Eq. 12)}$$

if

$$t > \frac{-\log(\Lambda_H) - \log(0.1)}{k_B}. \qquad \text{(Eq. 13)}$$

This result has profound implications for identifying hyporheic signals in traditionally obtained BTCs. The time required to identify the hyporheic signal can increase significantly with smaller hyporheic exchange and longer benthic residence. This equation also shows that the hyporheic signal time will be more sensitive to the benthic residence time than to the exchange rate with the subsurface because the benthic residence time scales linearly (i.e., faster) and the exchange rate scales logarithmically (i.e., slower).

The same approach considering a power-law RTD for the hyporheic zone does not yield an analytical solution. However, numerical evaluations show the greatest sensitivity to the k_B parameter. In the field, k_B can be estimated from a preliminary pulse injection and t can be estimated conservatively by taking a small value of Λ_H (e.g., 10^{-4}). Thus, the sampling time required to characterize hyporheic exchange can be estimated in the field. An important consequence is that this hyporheic signal time generally would be longer than the period of time over which data typically are acquired. Based on these results, we find that the short-term storage is primarily governed by surface and benthic processes, whereas actual hyporheic exchange takes much longer to appear. Harvey et al. (1996) suggested that between 6 and 8 travel times are needed for the short-term storage signal to vanish. This estimate is consistent with the findings of Drummond

et al. (2012) who recommended that data should be collected for >20 travel times to differentiate power-law and exponential tails.

Some investigators have speculated that long tails in in-stream BTCs occur because of tracer sorption in the subsurface, particularly with ionic tracers, such as Br^- and fluorescent organic tracers, such as Rhodamine (Bencala et al. 1983). Our results suggest that unless this sorption process is highly nonlinear, it is not likely to cause extended tailing in tracer studies. Linear sorption does lead to delays in the onset of these tails, but does not change their fundamental shape. Nonlinear sorption can produce power-law tails, but this effect is not significant until the isotherm becomes highly nonlinear (Freundlich exponents $<\sim 0.2$). Practically speaking, many injection experiments have used dyes that can sorb to sediments, but the sorption isotherm at the concentrations used in the field is usually linear, and never strongly nonlinear (Sutton et al. 2001, Gooseff et al. 2008). Thus, observed tailing can be attributed to processes other than sorption with some confidence. Simulating long-time storage as chemical retardation instead of hydrodynamic transport could lead to overestimation of the mean RTD (Gooseff et al. 2005) and a change in the shape of the BTC. These artifacts can be accounted for by measuring isotherms in batch experiments using sediments from the field. The model presented here can be adapted readily for any sorption isotherm to explicitly evaluate the effects of sorption on observed in-stream transport and, thereby, to obtain better estimates of stream transport parameters.

Interpretation of biogeochemical processes

Previous studies have clearly demonstrated the importance of hyporheic exchange for contaminant transport and nutrient dynamics (Holmes et al. 1996, Valett et al. 1996, Peterson et al. 2001, Boyer et al. 2006, Mulholland et al. 2008). As demonstrated in Figs 6A, B, and 7, subsurface uptake tempers power-law tails and dampens exponential tails. However, this tempering and dampening provide rich information that distinguishes between the rates of exchange between zones and the rates of uptake, provided that one can compare observations of conservative and reactive transport. Standard classical methods usually lump conservative and reactive tracers together to account for groundwater exchange, but valuable information about transport is lost (e.g., Fig. 8). A long tail in the BTC of the conservative solute combined with a tailless BTC for the reactive solute indicates transport limitation on net hyporheic uptake because extended residence time allows complete microbial uptake of the reactive tracer. In this case, the rate of removal of the reactive solute corresponds to the exchange rate with the hyporheic zone rather than the uptake rate (Kim et al. 1992). Conversely, distinct tempering of the tail of the reactive BTC relative to the conservative BTC reflects local uptake kinetics. When a power law is tempered by an exponential, i.e., the power-law behavior is altered by a superimposed exponential decay, the decay rate of the exponential is easy to obtain. If the tempering mechanism is solute uptake, then the uptake rate can be calculated directly by comparing the 2 curves. This comparison requires models that adequately represent the form of the conservative BTC and the effect of uptake on the tail of the reactive BTC. Our results suggest that co-injected conservative and reactive tracers can provide such information to measure the hyporheic reaction rate coefficient directly from the difference between the BTCs.

Subsurface data should be obtained, where feasible, to compare rates and time scales of exchange inferred from BTCs with direct local measurements (Duff et al. 1998, Harvey and Wagner 2000, Zarnetske et al. 2011). However, individual local observations are not necessarily expected to reflect reach-scale dynamics because of the high spatial variability in rivers, and BTC data provide the best estimate of upscaled whole-stream biogeochemistry. The major challenge is obtaining sufficient data to adequately characterize both tails without using such high tracer concentrations that they perturb or overwhelm the system. Use of isotopic tracers, such as ^{15}N and ^{3}H, greatly increases the sensitivity of injection experiments (Dodds et al. 2000, Wörman and Wachniew 2007, Mulholland et al. 2008, Drummond et al. 2012). Additions of reactive isotopes, such as ^{15}N, do not guarantee reliable results on their own because it is still important to understand the dynamics of delivery of these solutes to the microbial communities that use them. Thus, in short-term tracer-injection studies, it always is essential to compare the dynamics of a reactive tracer against a conservative tracer and to use an appropriate model framework to separate transport and transformation processes.

Hyporheic sorption delays solutes that enter the subsurface. Hyporheic sorption could be of particular significance for the transport of nutrients and estimation of their uptake. Both N and P are affected by sorption kinetics as they undergo both biological uptake and physicochemical sorption (House et al. 1995). Sorption to suspended and hyporheic sediments can be substantial, but biological uptake and physical transport to the bed also influence measured fluxes (Gächter and Meyer 1993), so that interpretation of bulk removal rates can also be misleading (Reddy et al. 1999). The CTRW, by representing both processes explicitly, can be used to allocate distinct rates for sorption, hyporheic exchange, and biological uptake.

Conclusions and implications

We have presented a novel model for reactive transport in rivers that accommodates arbitrary RTDs in the main stream channel, the benthic zone, and the hyporheic zone. We used the model to simulate the effects of transport, sorption, and 1^{st}-order uptake on downstream BTCs.

We showed that biological uptake alters RTDs of reactive solutes so that the long tails of associated in-stream BTCs are tempered at the time scale of the uptake kinetics. When both benthic and hyporheic signals are clearly identified, zone-specific uptake rates can be calculated from observations of coinjected conservative and reactive solutes, as shown here with a synthetic data set. A key finding is that in transport-limited systems, the hyporheic (or even benthic) signal may be entirely absent from the reactive tracer BTC. This result indicates that the hyporheic zone is potentially capable of consuming more mass than is delivered by hyporheic exchange, so that net uptake is transport limited. We also showed that linear sorption shifts BTC tails to later times without changing their shape and that sorption to sediments produces significant power-law tailing only when the reaction is highly nonlinear. Similar to the approach described for uptake, comparing conservative and sorptive solute BTCs can yield the isotherm exponents directly.

The underlying CTRW theory used here is general and allows the model assumptions to be relaxed as more information becomes available on particular transport and reaction processes. Improved knowledge of turbulent flow structure in the water column and across the interface will improve the assessment of transport, exchange, and storage processes, and clarify the physical meaning of the modeled storage zones. Similarly, more detailed observations of the spatial structure of biogeochemical processes in sediments and the coupling between multiple biogeochemical cycles can be used to improve the representation of reactions in reach-scale models. Improved upscaling of biogeochemical processes in watersheds will require explicit representations of nonstationary flow and morphology and a better understanding of the relationships between habitat and microbial community structure. Last, our results clearly demonstrate the influence of local transport and biogeochemical processes on reach-scale observations of reactive solute fluxes and provide a basis for improved interpretations.

ACKNOWLEDGEMENTS

This material is based upon work supported by the National Science Foundation under grant numbers EAR-0810270, -1344280, and -1351625. We also gratefully acknowledge support from the Water Cycle Dynamics in a Changing Environment hydrologic synthesis project (EAR-0636043), and from the Environmental Change Initiative at Notre Dame. RS received partial support from the Maki Chair of Hydrologic Sciences. We used the QUEST supercomputer at Northwestern and the Center for Research Computing high-performance computing resources at Notre Dame to generate some of the simulations in our paper.

LITERATURE CITED

Arfken, G. B., and H. J. Weber. 1995. Mathematical methods for physicists. 4th edition. Academic Press, San Diego, California.

Arnon, S., A. I. Packman, C. G. Peterson, and K. A. Gray. 2007. Effects of overlying velocity on periphyton structure and denitrification. Journal of Geophysical Research: Biogeosciences 112:G01002.

Bardini, L., F. Boano, M. Cardenas, A. Sawyer, R. Revelli, and L. Ridolfi. 2013. Small-scale permeability heterogeneity has negligible effects on nutrient cycling in streambeds. Geophysical Research Letters 84:47–61.

Battin, T. J., L. A. Kaplan, S. Findlay, C. S. Hopkinson, E. Martí, A. I. Packman, J. D. Newbold, and F. Sabater. 2008. Biophysical controls on organic carbon fluxes in fluvial networks. Nature Geoscience 1:95–100.

Bear, J. 1972. Dynamics of fluids in porous media. Elsevier, New York.

Bencala, K. E., R. E. Rathbun, A. P. Jackman, V. C. Kennedy, G. W. Zellweger, and R. J. Avanzino. 1983. Rhodamine WT dye losses in a mountain stream environment. Journal of the American Water Resources Association 19:943–950.

Bencala, K. E., and R. A. Walters. 1983. Simulation of solute transport in a mountain pool-and-riffle stream: a transient storage model. Water Resources Research 19:732–738.

Berkowitz, B., A. Cortis, M. Dentz, and H. Scher. 2006. Modeling non-Fickian transport in geological formations as a continuous time random walk. Reviews of Geophysics 44:RG2003.

Bernhardt, E. S., G. E. Likens, D. C. Buso, and C. T. Driscoll. 2003. In-stream uptake dampens effects of major forest disturbance on watershed nitrogen export. Proceedings of the National Academy of Sciences of the United States of America 100:10304–10308.

Boano, F., A. I. Packman, A. Cortis, R. Revelli, and L. Ridolfi. 2007. A continuous time random walk approach to the stream transport of solutes. Water Resources Research 43:W10425.

Bouchaud, J. P., and A. Georges. 1990. Anomalous diffusion in disordered media: statistical mechanisms, models and physical applications. Physics Reports 195:127–293.

Boyer, E. W., R. B. Alexander, W. I. Parton, C. Li, K. Butterbach-Bahl, S. D. Donner, R. W. Skaggs, and S. J. Del Gross. 2006. Modeling denitrification in terrestrial and aquatic ecosystems at regional scales. Ecological Applications 16:2123–2142.

Brutsaert, W. 2005. Hydrology: an introduction. Cambridge University Press, Cambridge, UK.

Butman, D., and P. A. Raymond. 2011. Significant efflux of carbon dioxide from streams and rivers in the United States. Nature Geoscience 4:839–842.

Cardenas, M. B., and J. L. Wilson. 2007. Hydrodynamics of coupled flow above and below a sediment–water interface with triangular bedforms. Advances in Water Resources 30:301–313.

Choi, J., J. W. Harvey, and M. H. Conklin. 2000. Characterizing multiple timescales of stream and storage zone interaction that affect solute fate and transport in streams. Water Resources Research 36:1511–1518.

Cirpka, O. A., M. N. Fienen, M. Hofer, E. Hoehn, A. Tessarini, R. Kipfer, and P. K. Kitanidis. 2007. Analyzing bank filtration by deconvoluting time series of electric conductivity, Groundwater 45:318–328.

De Anna, P., T. Le Borgne, M. Dentz, A. M. Tartakovsky, D. Bolster, and P. Davy. 2013. Flow intermittency, dispersion, and correlated continuous time random walks in porous media. Physical Review Letters 110:184502.

Delay, F., P. Ackerer, and C. Danquigny. 2005. Simulating solute transport in porous or fractured formations using random walk particle tracking: a review. Vadose Zone Journal 4:360–379.

Diaz, R. J., and R. Rosenberg. 2008. Spreading dead zones and consequences for marine ecosystems. Science 321:926–929.

Dodds, W. K., M. A. Evans-White, N. M. Gerlanc, L. Gray, D. A. Gudder, M. J. Kemp, A. L. Lopez, D. Stagliano, E. A. Strauss, J. L. Tank, M. R. Whiles, and W. M. Wollheim. 2000. Quantification of the nitrogen cycle in a prairie stream. Ecosystems 3:574–589.

Drummond, J. D., T. P. Covino, A. F. Aubeneau, D. Leong, S. Patil, R. Schumer, and A. I. Packman. 2012. Effects of solute breakthrough curve tail truncation on residence time estimates: a synthesis of solute tracer injection studies. Journal of Geophysical Research: Biogeosciences 117:G3.

Duff, J. H., F. Murphy, C. C. Fuller, F. J. Triska, J. W. Harvey, and A. P. Jackman. 1998. A mini drivepoint sampler for measuring pore water solute concentrations in the hyporheic zone of sand-bottom streams. Limnology and Oceanography 43: 1378–1383.

Elliott, A. H., and N. H. Brooks. 1997. Transfer of nonsorbing solutes to a streambed with bed forms: laboratory experiments. Water Resources Research 33:123–136.

Ensign, S. H., and M. W. Doyle. 2005. In-channel transient storage and associated nutrient retention: evidence from experimental manipulations. Limnology and Oceanography 50: 1740–1751.

Fischer, H., E. List, R. Koh, J. Imberger, and N. Brooks. 1979. Mixing in inland and coastal waters. Academic Press, San Diego, California.

Gächter, R., and J. S. Meyer. 1993. The role of microorganisms in mobilization and fixation of phosphorus in sediments. Pages 103–121 *in* Proceedings of the 3rd International Workshop on Phosphorus in Sediments. Springer, Dordrecht, The Netherlands.

Gooseff, M. N., J. LaNier, R. Haggerty, and K. Kokkeler. 2005. Determining in-channel (dead zone) transient storage by comparing solute transport in a bedrock channel–alluvial channel sequence, Oregon. Water Resources Research 41: 06014.

Gooseff, M. N., R. A. Payn, J. P. Zarnetske, W. B. Bowden, J. P. McNamara, and J. H. Bradford. 2008. Comparison of in-channel mobile–immobile zone exchange during instantaneous and constant rate stream tracer additions: implications for design and interpretation of non-conservative tracer experiments. Journal of Hydrology 357:112–124.

Grant, S. B., and I. Marusic. 2011. Crossing turbulent boundaries: interfacial flux in environmental flows. Environmental Science and Technology 45:7107–7113.

Haggerty, R., S. M. Wondzell, and M. A. Johnson. 2002. Power-law residence time distribution in the hyporheic zone of a 2nd-order mountain stream. Geophysical Research Letters 29. doi: 10.1029/2002GL014743.

Harvey, J., and B. J. Wagner. 2000. Quantifying hydrologic interactions between streams and their subsurface hyporheic zones. Pages 3–44 *in* J. B. Jones and P. J. Mulholland (editors). Streams and ground waters. Academic Press, San Diego, California.

Harvey, J. W., B. J. Wagner, and K. E. Bencala. 1996. Evaluating the reliability of the stream tracer approach to characterize stream-subsurface water exchange. Water Resources Research 32:2441–2451.

Hauer, R., and G. A. Lamberti. 2011. Methods in stream ecology. Academic Press, San Diego, California.

Hensley, R. T., and M. J. Cohen. 2012. Controls on solute transport in large spring-fed karst rivers. Limnology and Oceanography 57:912–924.

Holmes, R. M., J. B. Jones, S. G. Fisher, and N. B. Grimm. 1996. Denitrification in a nitrogen-limited stream ecosystem. Biogeochemistry 33:125–146.

House, W. A., F. H. Denison, and P. D. Armitage. 1995. Comparison of the uptake of inorganic phosphorus to a suspended and stream bed sediment. Water Research 29:767–779.

Kim, B. K., A. P. Jackman, and F. J. Triska. 1992. Modeling biotic uptake by periphyton and transient hyporheic storage of nitrate in a natural stream. Water Resources Research 28:2743–2752.

Margolin, G., M. Dentz, and B. Berkowitz. 2003. Continuous time random walk and multirate mass transfer modeling of sorption. Chemical Physics 295:71–80.

Marion, A., M. Zaramella, and A. Bottacin-Busolin. 2008. Solute transport in rivers with multiple storage zones: the STIR model. Water Resources Research 44:W10406.

Meerschaert, M. M. 2013. Mathematical modeling. Academic Press, San Diego, California.

Metzler, R., and J. Klafter. 2000. The random walk's guide to anomalous diffusion: a fractional dynamics approach. Physics Reports 339:1–77.

Mulholland, P. J., A. M. Helton, G. C. Poole, R. O. Hall, S. K. Hamilton, B. J. Peterson, J. L. Tank, L. R. Ashkenas, L. W. Cooper, C. N. Dahm, W. K. Dodds, S. E. G. Findlay, S. V. Gregory, N. B. Grimm, S. L. Johnson, W. H. McDowell, J. L. Meyer, H. M. Valett, J. R. Webster, C. P. Arango, J. J. Beaulieu, M. J. Bernot, A. J. Burgin, C. L. Crenshaw, L. T. Johnson, B. R. Niederlehner, J. M. O'Brien, J. D. Potter, R. W. Sheibley, D. J. Sobota, and S. M. Thomas. 2008. Stream denitrification across biomes and its response to anthropogenic nitrate loading. Nature 452:202–205.

Newbold, J. D., J. W. Elwood, R. V. O'Neill, and A. L. Sheldon. 1983. Phosphorus dynamics in a woodland stream ecosystem: a study of nutrient spiraling. Ecology 64:1249–1265.

O'Connor, B. L., and M. Hondzo. 2008. Dissolved oxygen transfer to sediments by sweep and eject motions in aquatic environments. Limnology and Oceanography 53:566–578.

Payn, R. A., M. N. Gooseff, D. A. Benson, O. A. Cirpka, J. P. Zarnetske, W. B. Bowden, J. P. McNamara, and J. H. Bradford. 2008. Comparison of instantaneous and constant-rate stream tracer experiments through non-parametric analysis of residence time distributions. Water Resources Research 44:W06404.

Peterson, B. J., W. M. Wollheim, P. J. Mulholland, J. R. Webster, J. L. Meyer, J. L. Tank, E. Martí, W. B. Bowden, H. M. Valett, A. E. Hershey, W. H. McDowell, W. K. Dodds, S. K. Hamilton, S. Gregory, and D. D. Morrall. 2001. Control of nitrogen export from watersheds by headwater streams. Science 292:86–90.

Rabalais, N. N., R. E. Turner, D. Justic, Q. Dortch, W. J. Wiseman, and B. K. Sen Gupta. 1996. Nutrient changes in the

Mississippi River and system responses on the adjacent continental shelf. Estuaries 19:386–407.
Raudkivi, A. J. 1979. Hydrology: an advanced introduction to hydrological processes and modeling. Pergamon Press, Oxford, UK.
Reddy, K. R., R. H. Kadlec, E. Flaig, and P. M. Gale. 1999. Phosphorus retention in streams and wetlands: a review. Critical Reviews in Environmental Science and Technology 29:83–146.
Salehin, M., A. I. Packman, and M. Paradis. 2004. Hyporheic exchange with heterogeneous streambeds: laboratory experiments and modeling. Water Resources Research 40:W11504.
Sawyer, A. H., and M. B. Cardenas. 2009. Hyporheic flow and residence time distributions in heterogeneous cross-bedded sediment. Water Resources Research 45:W08406.
Sawyer, A. H., M. B. Cardenas, and J. Buttles. 2011. Hyporheic exchange due to channel spanning logs. Water Resources Research 47:W08502.
Schumer, R., D. A. Benson, M. M. Meerschaert, and B. Baeumer. 2003. Fractal mobile/immobile solute transport. Water Resources Research 39. doi:10.1029/2003WR002141
Stonedahl, S. H., J. W. Harvey, J. Detty, A. Aubeneau, and A. I. Packman. 2012. Physical controls and predictability of stream hyporheic flow evaluated with a multiscale model. Water Resources Research 48(10):W10513.
Stream Solute Workshop. 1990. Concepts and methods for assessing solute dynamics in stream ecosystems. Journal of the North American Benthological Society 9:95–119.
Sutton, D. J., Z. J. Kabala, A. Francisco, and D. Vasudevan. 2001. Limitations and potential of commercially available rhodamine WT as a groundwater tracer. Water Resources Research 37:1641–1656.
Turner, R., and N. Rabalais. 1994. Coastal eutrophication near the Mississippi river delta. Nature 619–621.
Uma, K. O., B. C. E. Egboka, and K. M. Onuoha. 1989. New statistical grain-size method for evaluating the hydraulic conductivity of sandy aquifers. Journal of Hydrology 108:343–366.
Valett, H. M., J. A. Morrice, C. N. Dahm, and M. E. Campana. 1996. Parent lithology, surface-groundwater exchange, and nitrate retention in headwater streams. Limnology and Oceanography 41:333–345.
Wörman, A., and P. Wachniew. 2007. Reach scale and evaluation methods as limitations for transient storage properties in streams and rivers. Water Resources Research 43:10. doi:10.1029/2001WR000769
Zarnetske, J. P., R. Haggerty, S. M. Wondzell, and M. A. Baker. 2011. Dynamics of nitrate production and removal as a function of residence time in the hyporheic zone. Journal of Geophysical Research: Biogeosciences 116:G01025.